

Simulation Experiment and Acoustic Emission Study on Coal and Gas Outburst

Hui Li^{1,2} · Zengchao Feng² · Dong Zhao¹ · Dong Duan¹

Received: 24 February 2016 / Accepted: 11 April 2017 / Published online: 17 April 2017
© Springer-Verlag Wien 2017

Abstract A coal and gas outburst is an extreme hazard in underground mining. The present paper conducts a laboratory simulation of a coal and gas outburst combined with acoustic emission analysis. The experiment uses a three-dimensional stress loading system and a PCI-2 acoustic emission monitoring system. Furthermore, the development of a coal and gas outburst is numerically studied. The results demonstrate that the deformation and failure of a coal sample containing methane under three-dimensional stress involves four stages: initial compression, elastic deformation, plastic deformation and failure. The development of internal microscale fractures within a coal sample containing methane is reflected by the distribution of acoustic emission events. We observed that the deformation and failure zone for a coal sample under three-dimensional stress has an ellipsoid shape. Primary acoustic emission events are generated at the weak structural surface that compresses with ease due to the external ellipsoid-shaped stress. The number of events gradually increases until an outburst occurs. A mathematical model of the internal gas pressure and bulk stress is established through an analysis of the internal gas pressure and bulk stress of a coal sample, and it is useful for reproducing experimental results. The occurrence of a coal and gas outburst depends not only on the in situ stress, gas pressure and physical and mechanical characteristics of the coal mass but also on the free weak surface of the outburst

outlet of the coal mass. It is more difficult for an outburst to occur from a stronger free surface.

Keywords Acoustic emission · Coal and gas outburst · Ellipsoid · Numerical simulation · Three-dimensional stress

List of symbols

Θ	Bulk stress
σ_2	Confining stress
η	Instantaneous desorption rate
t	Time
n	Time effect divergence speed
B	Constant parameter
σ_Q	Coal mass strength of a free gas surface
q	Gas permeability
σ_h	Horizontal stress
σ_1	Axial stress
σ_3	Confining stress
η_{\max}	Final desorption rate
t_0	Median desorption time parameter
a	Constant parameter
p	Gas pressure
p_0	Atmospheric pressure
σ_v	Vertical stress

1 Introduction

A coal and gas outburst is a complex and severe mining hazard (Hu et al. 2015). Following an outburst, large quantities of coal blocks and gas are rapidly projected into a mine lane or onto a workplace. Mining lanes and equipment can be destroyed, and workers can be injured or killed. The frequency of coal and gas outburst accidents gradually increases with the depth of mining. Thus, it is

✉ Hui Li
13803439627@163.com

¹ College of Mining Engineering, Taiyuan University of Technology, Taiyuan, Shanxi, China

² Institute of Mining Technology, Taiyuan University of Technology, Taiyuan, Shanxi, China

difficult to conduct mining in a manner that is theoretically safe.

Researchers have proposed a synthesis hypothesis that a coal and gas outburst is caused by a combination of the in situ stress, gas pressure and physical mechanical characteristics of the coal (An and Cheng 2013). It is difficult to monitor or study the entire process of coal and gas outburst due to the extreme hazard that the outburst presents. Most research on the process has relied on physical, experimental and numerical simulation methods. The first physical experiments on coal and gas outburst were conducted by Skoczyński (1953) in the former Soviet Union. Next, other researchers began to simulate the process of coal and gas outburst in the laboratory using physical (Butt 1999; Chen et al. 2013; Sobczyk 2011; Lama and Bodziony 1998; Skoczylas 2012; Tu et al. 2016; Valliappan and Zhang 1999; Yin et al. 2013, 2016) and numerical (Xie et al. 2015; Perera et al. 2011a; Xue et al. 2011, 2014; Wang et al. 2012; Xu et al. 2006; Yang et al. 2011; Zhou et al. 2015) methods. Furthermore, the mechanism of coal and gas outburst has been analysed by employing a theoretical model (Beamish and Crosdale 1998; Choi and Wold 2001, 2004; Huang et al. 2010; Islam and Shinjo 2009; Perera et al. 2011b; Wu et al. 2009). Additionally, many researchers have studied microtremor monitoring and the law of acoustic emission development (Kong et al. 2016; Vishal et al. 2015) for the simulation of coal and gas outbursts.

The results of these studies have been used to further prevent coal and gas outbursts. However, problems remain; an outburst outlet was opened manually or mechanically to simulate a coal and gas outburst, and the change in gas pressure was studied less during the outburst process. To study the inner mechanism of a coal and gas outburst, including the generation, development and termination stages, the present paper conducts physical experiments on a coal and gas outburst using acoustic emissions. The three-dimensional simulation of a coal and gas outburst adopts experimental equipment that is manufactured by our research group. The equipment simulates not only the process of a coal and gas outburst under three-dimensional loading conditions but also the complete outburst when the outburst outlet is destroyed by coal and gas. During the outburst process, free weak surfaces easily rupture. The failure processes are monitored by employing acoustic emission technology under three-dimensional stress. The deformation and failure of a coal sample and the variation of the inner gas pressure during the outburst process are also studied. Finally, the coal and gas outburst development processes are simulated by employing numerical methods. This research is important for preventing coal and gas outbursts.

2 Experimental Methods

2.1 Preparation of Coal Samples and the Experimental Equipment

2.1.1 Preparation of Coal Samples

The coal samples used in the experiments were acquired from the tunnelling working face 15,203 of the Yangquan Coal Group, Ltd., in Shanxi Province, China. The gas content of the coal was $11.22 \times 10^{-3} \text{ m}^3/\text{kg}$, the bulk density was $1.4 \times 10^3 \text{ kg/m}^3$, the modulus of elasticity was 4.7 GPa, the compressive strength was 21.2 MPa, the tensile strength was 2.7 MPa, the Poisson's ratio was 0.24, and the porosity was 3.01%. The samples were crushed and vibrated, and the particles with diameters $>2 \text{ mm}$ were automatically sieved out. The remaining samples were injected with 3% water, which is the moisture content of raw coal. The samples were stirred without a gelatinizer, placed into a mould and compressed repeatedly. The dimensions of a modelled coal sample were $100 \text{ mm} \times 100 \text{ mm} \times 100 \text{ mm}$. The samples were compressed under 25 MPa pressure for approximately 1 h and then kept at $90 \text{ }^\circ\text{C}$ and 25 MPa for approximately 6 h. The test samples of coal are presented in Fig. 1.

2.1.2 Experimental Equipment

The experiments adopted equipment that loaded a three-dimensional stress on samples for the simulation of coal and gas outburst. The equipment comprised a system for coal and gas outburst simulation, a system for the loading and monitoring of the dynamic pressure and a system for adsorbing and monitoring the methane. The apparent dimensions of the system for the coal and gas outburst simulation were 230 mm (diameter) \times 300 mm (length), while the inner dimensions of the simulation system were 145 mm (diameter) \times 200 mm (length). In the simulation system, a rubber cover was placed over the coal sample with dimensions of $100 \text{ mm} \times 100 \text{ mm} \times 100 \text{ mm}$. One side of the sample was a free weak surface that played the role of an outlet, while the opposite side was connected to the system that was used for the loading and monitoring of the dynamic pressure. Three-dimensional dynamic stresses were loaded via a hydraulic system, while pressure gauges and a regulating valve were used for data collection and monitoring. A methane adsorption and monitoring system monitored the gas adsorption and gas pressure. A CH_4 (99.99% concentration) gas bottle was used in the system. Gas was injected into the coal sample through the central zone, and the stresses in different directions were loaded separately. The equipment used for the simulation of the coal and gas outburst is presented in Fig. 2.

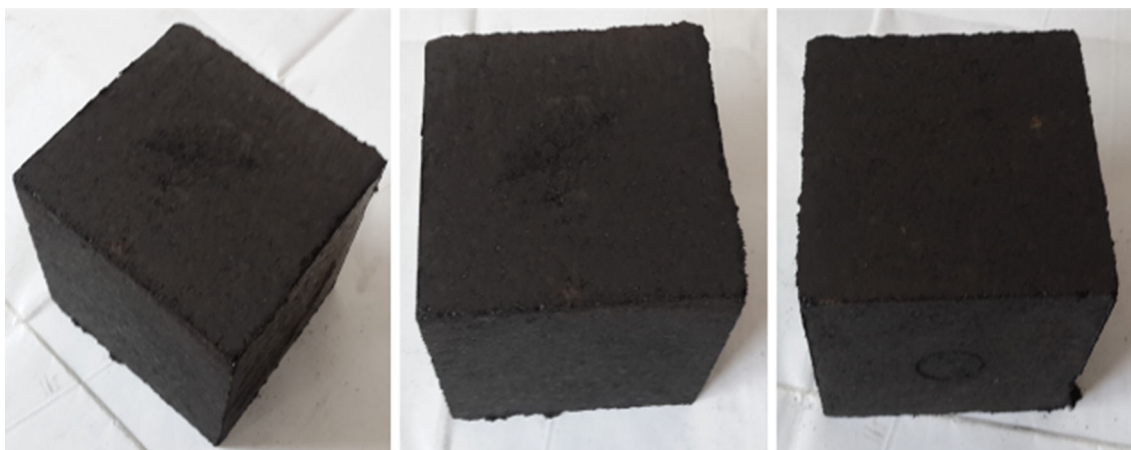


Fig. 1 Test samples of coal

A PCI-2 acoustic emission testing system manufactured by the American Emission Physical Company was adopted. This system monitored the generation and evolution of the coal and gas outburst. To monitor the entire process for the coal sample from microcosmic to failure unsteady and to eliminate calculation errors of the fixed position of the acoustic emission caused by the deformation of the coal sample during the loading process, the experiments

adopted innovative techniques such as the three-dimensional fixed position of the acoustic emission, various arrangement methods before the experiments to obtain the most suitable arrangement, and 4-pass three-dimensional orthogonality. These arrangements were effective for observing the acoustic emission events of deformation and failure from the coal sample and allowed the three-dimensional fixed-position monitoring of the acoustic emission events.

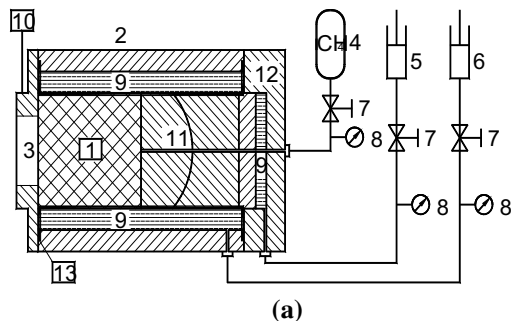


Fig. 2 Experimental equipment for the simulation of coal and gas outburst. **a** Principle diagram of experimental equipment for the simulation of coal and gas outburst, **b** apparent of the simulation of coal and gas outburst. 1 The coal sample; 2 simulation system of coal and gas outburst; 3 free weak surface of the outburst outlet; 4 CH₄ gas bottle; 5 axial stress loading equipment; 6 confining stress loading equipment; 7 regulating valve; 8 pressure gauge; 9 liquid medium; 10 acoustic emission testing system; 11 spherical seat; 12 load cylinder; 13 rubber case

2.2 Experimental Conditions and Procedure

2.2.1 Experimental Conditions

Based on the test results of the coal bed gas pressure, three initial gas pressures of 0.65, 0.70 and 0.75 MPa were adopted in the physical simulation. Meanwhile, based on similar strength materials of the free weak surface of the outburst outlet, materials that had the same strength as the coal sample were adopted. The similar materials had strengths of 18, 20, 22 and 24 MPa and low gas permeability.

The physical simulation was conducted under the same confining pressure of the three-dimensional stress. The bulk stress for the coal sample containing methane was combined and analysed. The bulk stress is expressed as

$$\Theta = \sigma_1 + \sigma_2 + \sigma_3 \tag{1}$$

where Θ is the bulk stress of the coal sample, σ_1 is the axial stress, and σ_2 and σ_3 are confining stresses that have the same amplitude.

In the experiments, $\sigma_2 = \sigma_3$, and thus Eq. (1) can be simplified as

$$\Theta = \sigma_1 + 2\sigma_2 \tag{2}$$

The conditions in the experimental runs are presented in Table 1.

Table 1 Conditions in the experimental runs

Experiment no.	Initial gas pressures (MPa)	Free weak surface of the outburst outlet strength (MPa)	Bulk stress of coal sample for outburst completed (MPa)
TI	0.65	18	46
TII	0.65	20	50
TIII	0.65	22	56
TIV	0.65	24	65
TV	0.70	18	44
TVI	0.70	20	49
TVII	0.70	22	54
TVIII	0.70	24	62
TIX	0.75	18	42
TX	0.75	20	46
TXI	0.75	22	51
TXII	0.75	24	56

The threshold value of the testing system was 40 dB, the gain of the first amplifier was 40 dB, the simulation filter bandwidth ranged from 20 kHz to 1 MHz, and the sampling frequency was 1 MSPS. The data were collected and analysed using the AEWin for PCI-2 software.

2.2.2 Experimental Procedure

The first step in the experiment was the preparation of the coal sample under standard conditions. The second step was placing the sample into the experimental equipment and setting and sealing the equipment. The system used for loading and monitoring the dynamic pressure was connected to the accessory equipment at this time. The third step was applying a vacuum to the coal sample and closing the valve. The adsorption equipment and monitoring system were opened and connected to the CH₄ gas bottle, and the gas pressure was allowed to stabilize over a period of 24 h. The fourth step was loading the three-dimensional stress using the dynamic stress loading and testing systems, and the final step was collecting and analysing the experimental data. The procedure was then repeated for each new sample.

3 Experimental Results and Analysis

3.1 Analysis of the Deformation and Failure Characteristics of a Coal Sample Under Three-Dimensional Stress

To simulate the entire outburst process of a coal sample containing methane under in situ stress and gas pressure, the free weak surface of the outburst outlet was taken as the

failure location, and the axial and confining pressures were increased in intervals of 2 MPa under the initial stress state of coal containing gas at the same time, and the bulk stress was increased in intervals of 6 MPa. The next loading was applied after the acoustic emission events became steady (i.e. at an interval of 1 min). The loading of the coal containing gas continued until there was a coal and gas outburst, and the parameters of the different stress loading phases were monitored and recorded throughout the experiment. The coal sample broke apart under three-dimensional stress, and acoustic emission events were then generated. Figures 3, 4 and 5 show the acoustic emission distribution and parameter characteristics during the deformation and failure of a coal sample. The data were collected using the acoustic emission testing system.

Figures 3, 4 and 5 show that the coal sample containing methane underwent deformation, failure and then outburst and that there was a subsequent increase in the bulk stress. According to the number of acoustic emission events, the positions of emission events, the changes in the frequency of the occurrence of emission events and the degree of sample failure under three-dimensional stress, the process of a coal and gas outburst can be divided into four stages by combining the time and space distributions and characteristics of acoustic emissions.

The first stage was the initial compressive stage. Acoustic emission events occurred under three-dimensional stress, but there were few events, and the change in the occurrence rate was slight, with the number of events increasing by 5 per 10 s, as shown by curve A in Fig. 3. The emission events mostly occurred at the weak structural surface, far from the centre of the coal sample. The zone of events had a shape similar to that of a semi-ellipsoid, as shown in Fig. 4. The count number, energy and energy rate were all low. The energy increased slowly, while the amplification range was small, as shown in Fig. 5. This property is observed because the coal mass has pores and fractures, as well as many raw fractures and joints, and thus, there were weak structural surfaces in the coal mass. In this stage, for the coal sample containing methane under three-dimensional stress, the raw fractures closed and became condensed, and new fractures formed. Additionally, new fractures formed at the weak structural surface, which readily failed under stress. However, the coal mass did not fail.

The second stage was the elastic deformation stage. There was an obvious increase in the number of acoustic emission events, followed by an increase in the bulk stress, and the frequency of the acoustic emissions gradually increased. The number of acoustic emission events increased by 11 per 10 s, as shown by curve B in Fig. 3. There were an increasing number of events around the sample centre. The semi-ellipsoidal zone of the events

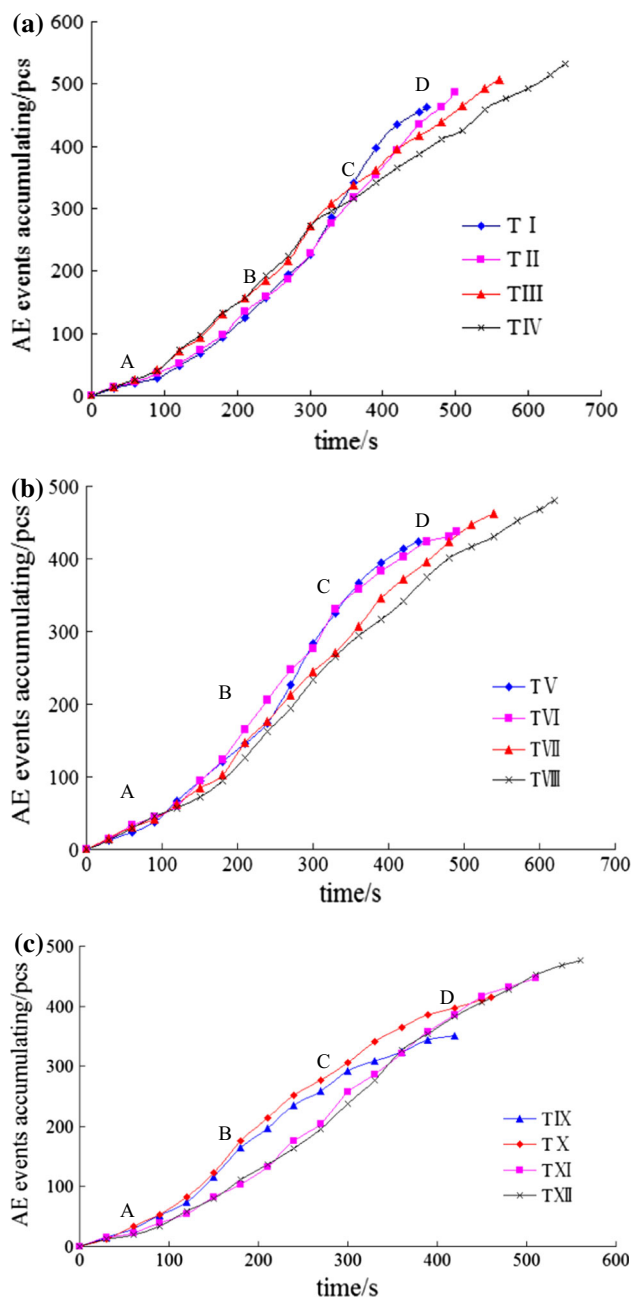


Fig. 3 Temporal distributions of accumulated acoustic emission events in the coal sample. **a** Initial gas pressure is 0.65 MPa, **b** initial gas pressure is 0.70 MPa, **c** initial gas pressure is 0.75 MPa. **A** Initial compressive stage; **B** elastic deformation stage; **C** plastic deformation stage; **D** failure stage

gradually enlarged, as shown in Fig. 4, and the free weak surface of the outburst outlet was externally expanded. The count number and energy rate increased, and the amplification range gradually increased and was occasionally large, as shown in Fig. 5. These results were due to raw fractures being compressed and expanded, new fractures emerging and growing, and the coal sample containing methane expanding and being distributed under three-

dimensional stress. The sample began to deform and fail. The occasional large range of the energy increase was due to the formation of new fractures and the expansion of raw fractures.

The third stage was the plastic deformation stage. The acoustic emission events increased in number, and there was a subsequent increase in the bulk stress. However, the increase in velocity gradually slowed, and the number of events increased by 5 per 10 s, as shown by curve C in Fig. 3. The semi-ellipsoidal shape of the zone of events expanded, as shown in Fig. 4, as did the free weak surface of the outburst outlet. The count number and energy rate were constant, and the energy gradually increased to a steady level. The amplification range was steady, as shown in Fig. 5. These results were due to many new fractures forming, combining, and connecting. Thus, the corresponding effects were enhanced. Semi-fractures formed throughout the sample, except at the primary failure surface. The coal mass gradually faulted and failed, and the bulk stress subsequently increased.

The fourth stage was the failure stage. The acoustic emission events slowly increased in number by 3 per 10 s, as shown by curve D in Fig. 3. The count number and energy rate were steady, and the energy slowly increased, as shown in Fig. 5. This is because many fractures that were connected expanded and extended, the failure zone reached a maximum size, and an outburst occurred. Finally, there was a coal and gas outburst at the free weak surface under the combined effects of the in situ stress and gas pressure, as shown in Fig. 4.

Overall, a coal and gas outburst is a failure process of energy accumulation and coal deformation under three-dimensional stress, and the degree of failure increases with the magnitude of the three-dimensional stress. In the experiments, once the accumulated energy reached the failure limit of the free weak surface, the failure of the surface was inevitable, and there was a coal and gas outburst. The failure zone had a shape similar to a semi-ellipsoid. Acoustic emission events first occurred at the weak structural surface far from the sample centre, and then, the number of events gradually increased. The deformation and degree of failure of the coal sample also increased gradually, finally resulting in an outburst. The failure zone became a large semi-ellipsoid in which approximately 83.8–90.9% of the events occurred. Figure 6 is a profile of the distribution of the accumulated acoustic emission events after the deformation and failure. By injecting liquid gypsum into the outburst zone after the experiments, three-dimensional actual failure zones were seen after gypsum solidification, as shown in Fig. 7.

Figure 7 shows that the outburst coal was a semi-ellipsoid zone from the former coal sample. Thus, the acoustic emission research has demonstrated that the

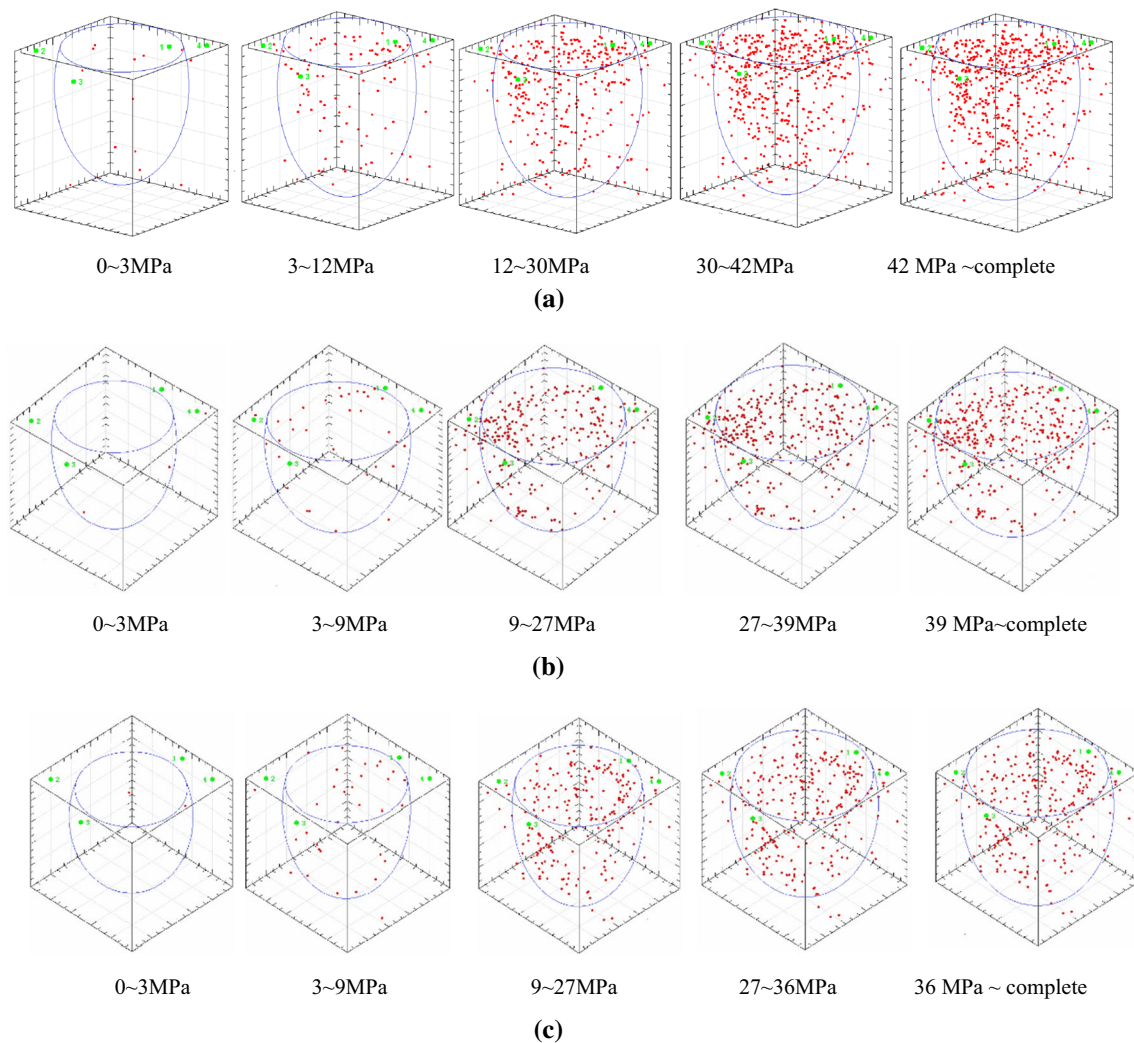


Fig. 4 Spatial distributions of accumulated acoustic emission events in the coal sample. **a** Initial gas pressure is 0.65 MPa, **b** initial gas pressure is 0.70 MPa, **c** initial gas pressure is 0.75 MPa

failure zone takes a semi-ellipsoidal shape, as predicted theoretically.

Because of the modelling of the physical experiments and setting of acoustic emissions, the present study focused on the deformation and failure of a coal sample and not of a free weak surface. According to the analysis of the physical simulation results and acoustic emission characteristics, an approximately semi-ellipsoidal zone was obtained after the failure. However, the failure zone of a coal mine outburst is actually a small side big body. Considering the physical and mechanical characteristics of the coal and rock, the deformation of the free weak surface throughout the outburst process under three-dimensional stress, the approximately semi-ellipsoidal zone after failure found by acoustic emission monitoring and the actual three-dimensional failure model after an outburst, we find that the deformation and failure zone of a coal sample containing methane under three-dimensional stress is a semi-ellipsoid.

3.2 Physical Simulation

3.2.1 Analyses of Gas Pressure Variation of a Coal Sample

According to the design of the experimental equipment of the physical simulation, a material with low gas permeability was selected as the free weak surface of the outburst outlet. The relationship among the bulk stress of the coal, internal gas pressure of the coal and outburst outlet strength of the coal rock mass was studied during the process of the coal and gas outburst.

In a gas-permeable coal seam, the adsorbed gas in the coal began to desorb under the effect of the bulk stress, and the gas flow in the coal particles obeys Darcy's law. According to the Airey (1968) relationship for the change in the capacity of gas desorption with time, the relationship between the coal desorption rate and time is

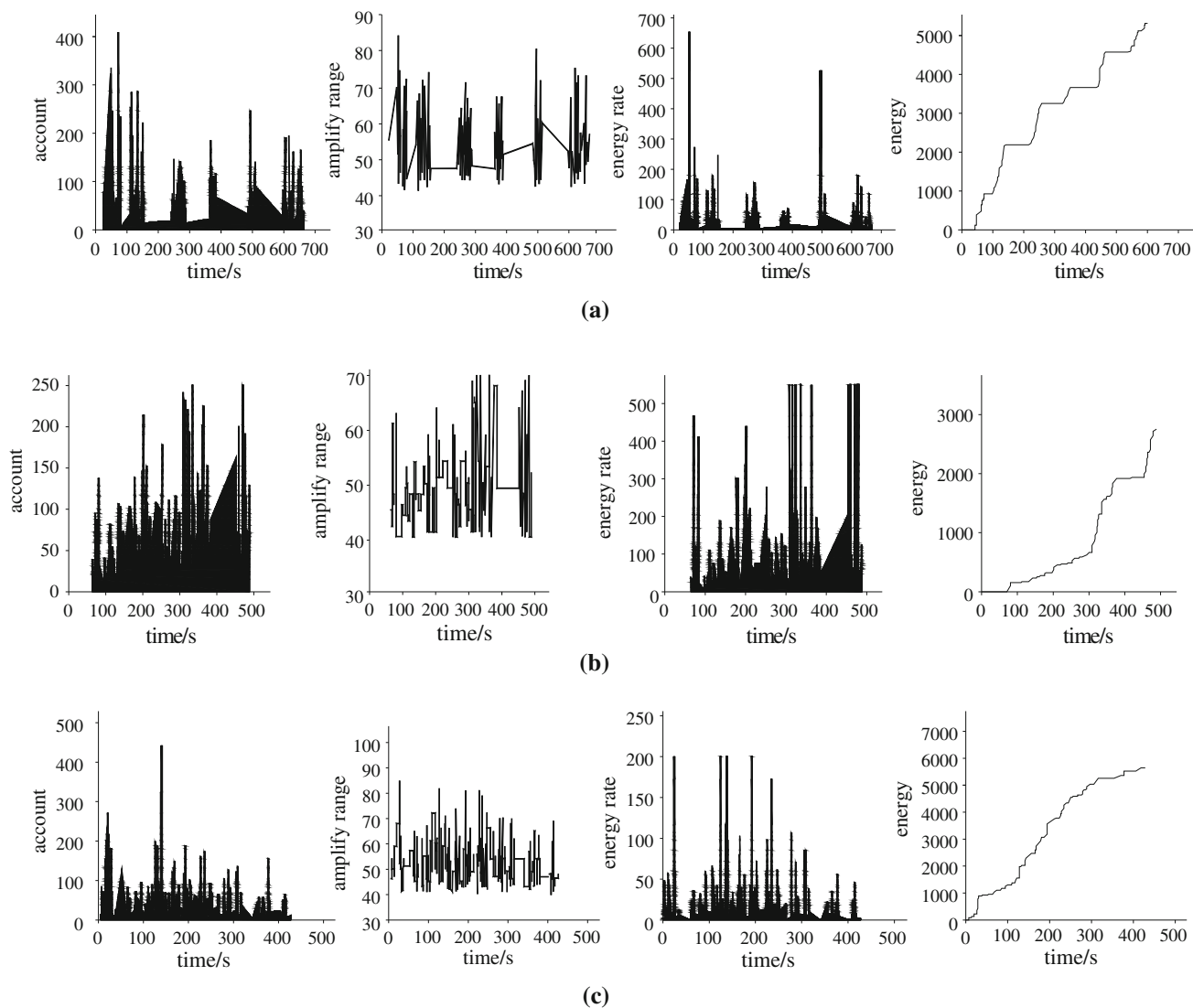


Fig. 5 Characteristics of acoustic emissions during the deformation and failure of a coal sample. **a** Initial gas pressure is 0.65 MPa, **b** initial gas pressure is 0.70 MPa, **c** initial gas pressure is 0.75 MPa

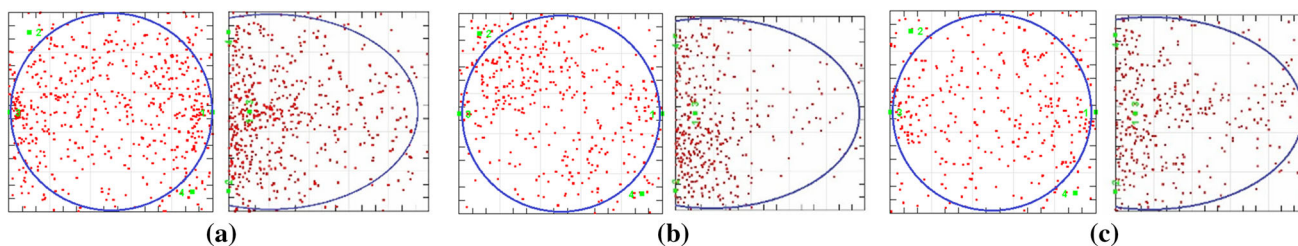


Fig. 6 Profile of the distribution of accumulated acoustic emission events after deformation and failure. **a** Initial gas pressure is 0.65 MPa, **b** initial gas pressure is 0.70 MPa, **c** initial gas pressure is 0.75 MPa

$$\eta = \eta_{\max} \left\{ 1 - \exp \left[- \left(\frac{t}{t_0} \right)^n \right] \right\} \tag{3}$$

$$\eta = \eta_{\max} \left(1 - \frac{a\Theta}{1 + b\Theta} \right) \tag{4}$$

According to the Langmuir (1917) formula for isothermal adsorption and desorption, the relation between the desorption rate and bulk stress of coal is

where η is the instantaneous desorption rate, η_{\max} is the final desorption rate, t is the time, t_0 is the median

Fig. 7 Actual three-dimensional failure zones after an outburst



desorption time parameter, n is the time effect divergence speed, and a and b are constant parameters.

The experimental results of the present study show that the deformation and failure of a coal sample under three-dimensional stress was such that the inner fractures increased in number, expanded and connected, and there was a subsequent increase in the bulk stress. The adsorbed gas in the coal began to desorb, the coal strength subsequently decreased, and the desorption velocity gradually increased. A significant amount of the desorption gas moved to a low-pressure zone, which was the free weak surface of the outburst outlet. An outburst occurred once the comprehensive stress of the coal reached the strength of the free weak surface. Employing the least-squares method, regression analyses were adopted for the gas pressure as a function of the bulk stress. The mathematical model of the gas pressure and bulk stress is

$$p = k_0 \Theta^m \quad (5)$$

where p is the gas pressure in the coal, and k_0 is a constant parameter.

The gas pressure in the coal is shown as a function of the bulk stress in Fig. 8. The simulation results and coefficient index are presented in Table 2.

Figure 8 and Table 2 reveal that the inner gas pressure increases with the bulk stress throughout the development of the coal and gas outburst. These values are well fitted by the external bulk stress, with all coefficient indexes exceeding 0.9744. This demonstrates that the inner gas pressure of the coal is nonlinearly related to the bulk stress, with a high coefficient index throughout the outburst process.

Considering the actual production in a coal mine, a coal mass containing methane would be destroyed by the comprehensive stresses in mines facing coal and gas

outburst hazards. During the outburst process, the inner fractures increase in number, the strength decreases, the gas undergoes desorption, and some of the adsorbed gas becomes free gas. The manual production and surrounding rock permeability are significantly less than the coal mass permeability due to the gas accumulation caused by the free gas not being removed. The gas pressure in the coal mass increases gradually due to the comprehensive stresses, and it may move to a low-pressure area. Because the free weak surface of the outburst is only affected by the atmosphere, there is a large difference between the inner gas pressure and atmospheric pressure. Finally, the free weak surface is destroyed, and a coal and gas outburst occurs.

3.2.2 Analysis of the Relationship Between the Coal Mass Bulk Stress and the Coal Mass Strength of the Free Weak Surface

A coal mass was destroyed under three-dimensional stress in the present experiments. Figure 9 shows the relationship between the strength of the free weak surface and the bulk stress of the coal mass at different initial gas pressures.

A mathematical model of the bulk stress of the coal mass and the strength of the free weak surface is established from the experimental results,

$$\Theta = k_1 \text{Exp}(k_2 \sigma_Q) \quad (6)$$

where σ_Q is the strength of the free weak surface of the coal mass, and k_1 and k_2 are constant parameters.

The simulation results and coefficient indexes are presented in Table 3.

Figure 9 and Table 3 reveal that the bulk stress fits the strength of the free weak surface well, with all coefficient

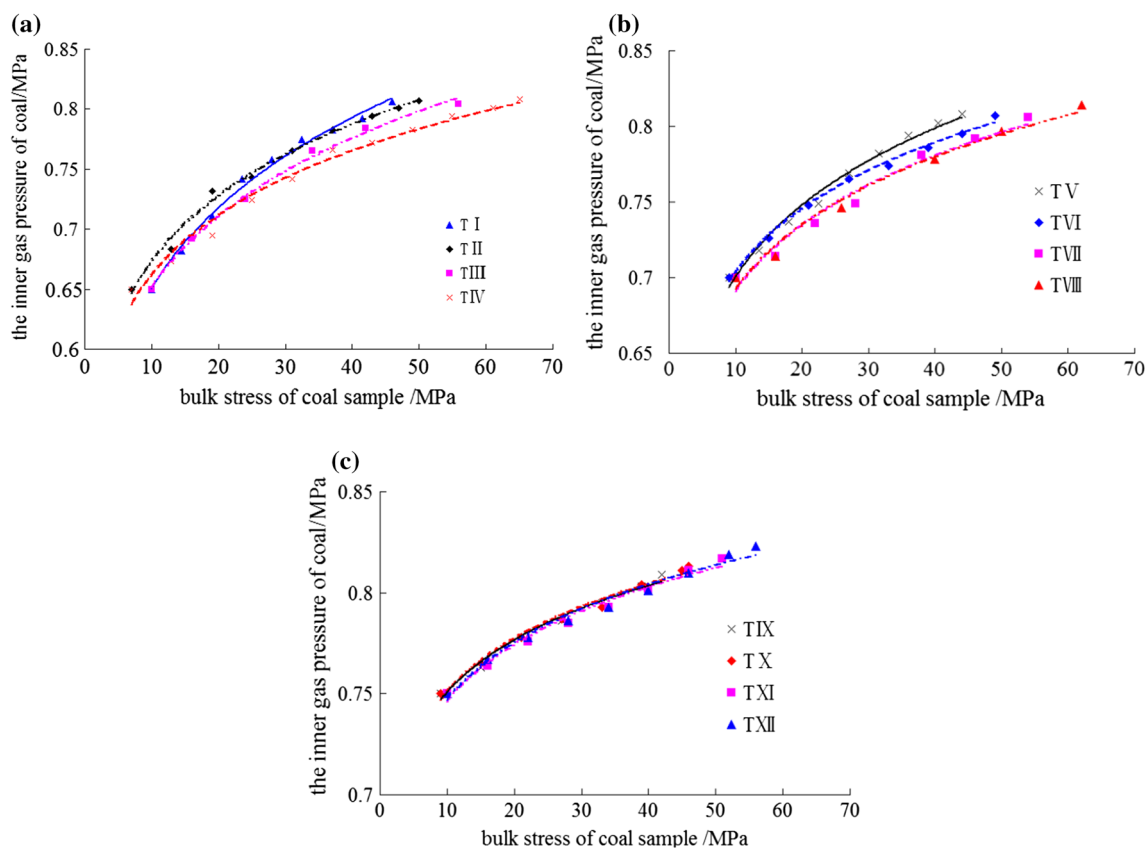


Fig. 8 Curves of gas pressure in coal followed by bulk stress. **a** Initial gas pressure is 0.65 MPa, **b** initial gas pressure is 0.70 MPa, **c** initial gas pressure is 0.75 MPa

Table 2 Simulation results and coefficient index

Experiment no.	Initial gas pressure (MPa)	Free weak surface of the outburst outlet strength (MPa)	Simulation results	Coefficient index
TI	0.65	18	$p = 0.4680\Theta^{0.1430}$	0.9937
TII	0.65	20	$p = 0.5186\Theta^{0.1132}$	0.9907
TIII	0.65	22	$p = 0.4869\Theta^{0.1263}$	0.9962
TIV	0.65	24	$p = 0.5203\Theta^{0.1046}$	0.9819
TV	0.70	18	$p = 0.5633\Theta^{0.0947}$	0.9877
TVI	0.70	20	$p = 0.5823\Theta^{0.0824}$	0.9959
TVII	0.70	22	$p = 0.5649\Theta^{0.0877}$	0.9744
TVIII	0.70	24	$p = 0.5686\Theta^{0.0856}$	0.9834
TIX	0.75	18	$p = 0.6710\Theta^{0.0489}$	0.9866
TX	0.75	20	$p = 0.6705\Theta^{0.0494}$	0.9882
TXI	0.75	22	$p = 0.6617\Theta^{0.0524}$	0.9852
TXII	0.75	24	$p = 0.6616\Theta^{0.0529}$	0.9836

indexes exceeding 0.9840. At the same initial gas pressure, the minimum bulk stress that is required for a coal and gas outburst to occur increases with the strength of the free weak surface. If the comprehensive stress required to destroy the free weak surface is reached, an outburst occurs. At the same time, for one fixed outburst, the bulk stress decreases as the initial gas pressure increases.

Considering the actual production in a coal mine, an outburst does not occur even if the external comprehensive stress is stable and the initial gas pressure is high. However, in the case of manual production that redistributes the in situ stresses, the coal mass is destroyed, the gas pressure increases, and a coal and gas outburst occurs. The comprehensive stress increases with the depth, and therefore,

coal and gas outbursts primarily occur in outburst hazard coal mines. Manual production redistributes the comprehensive stress, so the inner gas pressure increases, and the external stress subsequently increases. If the free gas cannot be removed, a coal and gas outburst occurs at the free weak surface under comprehensive stress.

Overall, the occurrence of a coal and gas outburst depends not only on the gas pressure, in situ stresses and physical and mechanical characteristics of the coal mass, but also on the rock characteristics of the free weak surface. Thus, a coal mass is destroyed under external stress during the development of a coal and gas outburst. An outburst occurs if the comprehensive stress exceeds the strength of the free weak surface. This is the primary external stress causing an outburst to occur, as the gas pressure gradually increases under an external stress.

3.3 Numerical Simulations

3.3.1 Establishing a Numerical Model

Numerical calculations are widely adopted in engineering academia. A numerical simulation combines a mechanical method with a numerical calculation method. Considering the heterogeneity of the rock characteristics, material properties are assigned to a given Weibull distribution, and an elastic finite element method is adopted to analyse the stress field of the research object. The mechanical parameters of the material satisfy the elastic damage constitutive relation. When the unit stress reaches the maximum tensile stress criterion or the Mohr–Coulomb criterion, the initial damage is considered to undergo a damage evolution according to the elastic damage constitutive relation.

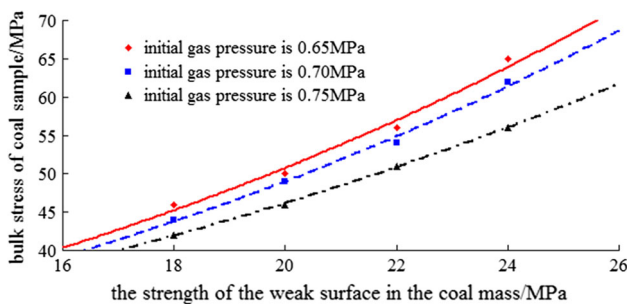


Fig. 9 Relationship between the strength of the free weak surface in the coal mass and the bulk stress

Table 3 Simulation results of the coal mass bulk stress and strength of the free weak surface

No.	Initial gas pressure (MPa)	Simulation results	Coefficient index
1	0.65	$\Theta = 16.071\text{Exp}(0.0575\sigma_Q)$	0.9840
2	0.70	$\Theta = 15.891\text{Exp}(0.0563\sigma_Q)$	0.9943
3	0.75	$\Theta = 17.572\text{Exp}(0.0483\sigma_Q)$	0.9995

Based on these assumptions, to simulate the uncovering of rock cross-cut coal to induce the development of a coal and gas outburst, the mechanism of the coal and gas outburst process was studied, and a two-dimensional numerical model was established, as shown in Fig. 10. There is a fixed-width rock seam at the front of a coal seam, and the gas pressure is equal to the atmospheric pressure at the front of the rock seam. To simulate a tunnelling working face to the next circle, the external stress is gradually increased until an outburst occurs.

In the analysis of the platform strain, the model has dimensions of 15 m × 10 m and is divided into 300 × 200 units. From top to bottom, there is a cover platform of 4 m depth, a coal seam of 3 m depth and a bottom platform of 3 m depth. The permeabilities of the cover and bottom platforms are both low, i.e. $q = 0$. On the left of the tunnelling working face is a free weak surface, where the gas pressure is equal to the atmospheric pressure, and on the right of the tunnelling working face is a coal seam in which the gas pressure is 0.7 MPa. The elastic modulus and compression strength of the cover and bottom platforms are both greater than those of the coal seam. The basic parameters of the numerical model are given in Table 4.

3.3.2 Results and Analysis of Numerical Simulation

The initial horizontal stress is 2 MPa, and the initial vertical stress is 2 MPa. At the beginning of the numerical simulation, the model is dipped 20 units once the tunnelling working face forces a circle. The stress changes in intervals of 2 MPa. Figure 11 shows the simulation of the

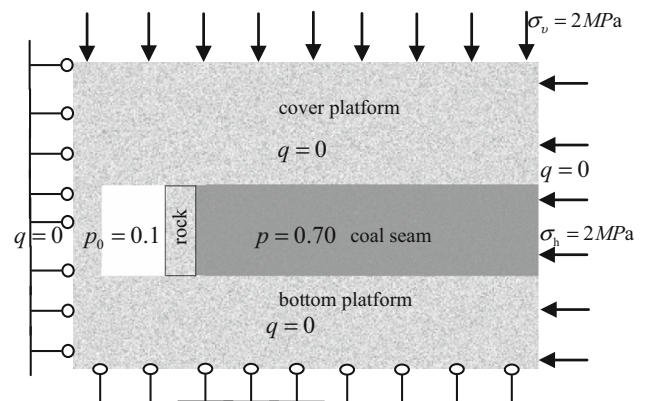


Fig. 10 Two-dimensional numerical model

Table 4 Basic parameters of the numerical model

No.	Mechanical parameters	Coal seam	Cover and bottom platform
1	Heterogeneity	3	10
2	Elastic modulus (GPa)	5	50
3	Compressive strength (MPa)	22	200
4	Poisson ratio	0.24	0.25
5	Permeability coefficient (m ² /MPa ² d)	0.18	0.001
6	Coefficient of gas content	2	0.001
7	Coefficient of pore pressure	0.5	0.001

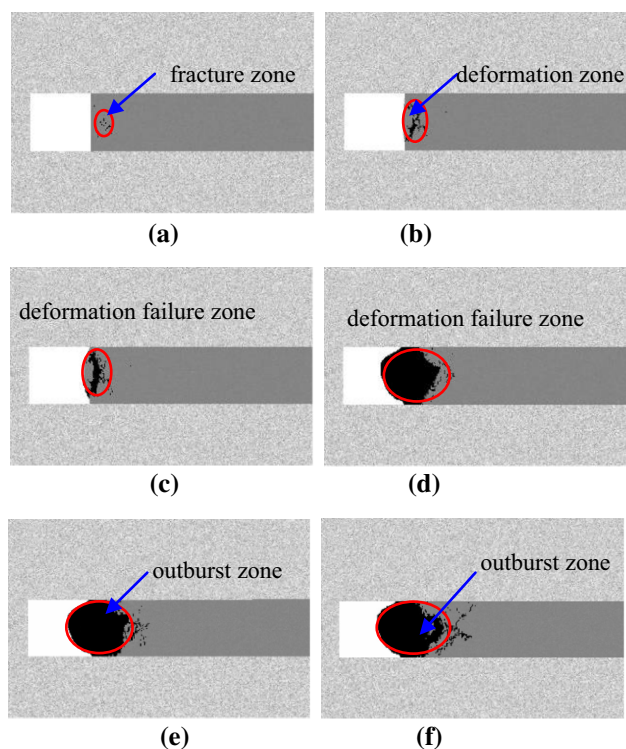
coal and gas outburst followed by stress accumulation after the start of production. Figure 12 presents curves of the gas pressure distribution for the forward working face followed by an increase in the stress. Figure 13 presents the stress distribution curves for the forward working face during the outburst process.

In Figs. 11, 12, and 13, the free weak surface is varied by dipping the model a certain number of units, and new free weak surfaces are produced. The stress of the forward working face of the coal seam is then distributed. The coal mass is destroyed, there is subsequent loading and an increase in stress, and an outburst finally occurs. There are four stages of coal and gas outburst that are based on the variation of the free weak surface, the inner deformation and failure of the coal mass, the variation of the gas pressure and the development of the coal seam stress.

The first stage corresponds to the stress that is in the range of the initial pressure to 8 MPa. The coal mass is compressed because of its homogeneity and double medium porous structure. Fractures form near the free weak surface and gradually produce an approximately ellipsoidal zone. The coal mass is complete and undamaged, as shown in Fig. 11a. There is an obvious gap in the gas pressure at the front of the working face, the range of which is 0.6 m, as shown by curve A in Fig. 12.

The second stage is the failure of the coal mass once the stress reaches 10.4 MPa. The fractures increase in number, expand and connect. The gas in the coal is desorbed, while the stress varies, and the number of fractures increases. The free gas increases in volume and moves to a low-pressure zone. The pressure gap range reaches 1.0 m in front of the coal wall, as shown by curve B in Fig. 12. The stress that acts on the coal mass is primarily from the main compression stress to the gas dynamic process. The deformation zone is semi-ellipsoidal, as shown in Fig. 11b.

The third stage is the generation and expansion of a new free weak surface once the stress reaches 11.6 MPa. More new fractures form, expand and connect, and the amount of free gas increases and fully fills the coal mass. There is a large gap between the inner coal mass and the free weak surfaces, as shown by curve C in Fig. 12. The range of the gas pressure gap and gas moving stress increase, and the

**Fig. 11** Numerical simulation of a coal and gas outburst

zone of deformation failure becomes larger. The ellipsoidal zone is basically formatted, as shown in Fig. 11c.

The fourth stage is the merging of the maximum failure zone once the stress reaches 12.4 MPa. The blocked coal and gas are ejected rapidly, and the deformation failure zone takes the shape of a large ellipsoid, as shown in Fig. 11d. The gas is desorbed and forms a maximum gas pressure gap, as shown by curve D in Fig. 12. Under the strain and compressive stress, the peak value of the stress moves into the inner coal seam, and deformations occur, as shown in Fig. 13. This causes a coal and gas outburst.

The above results reveal that the in situ stresses are distributed during a coal and gas outburst under the effects of the in situ stress, gas pressure and manual production. The peak stress of the coal mass moves into the inner coal seam, and the coal mass fails, and its strength decreases. New

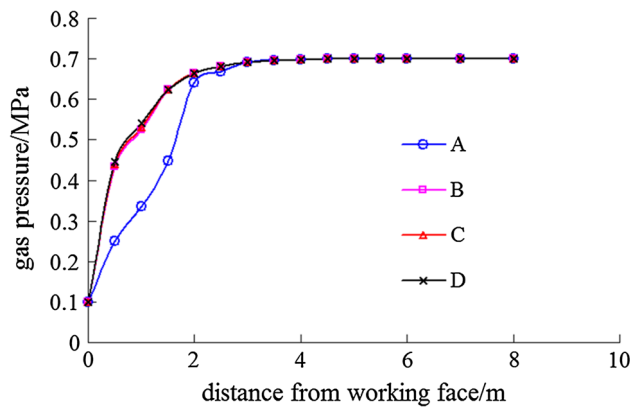


Fig. 12 Gas pressure distribution for the forward working face

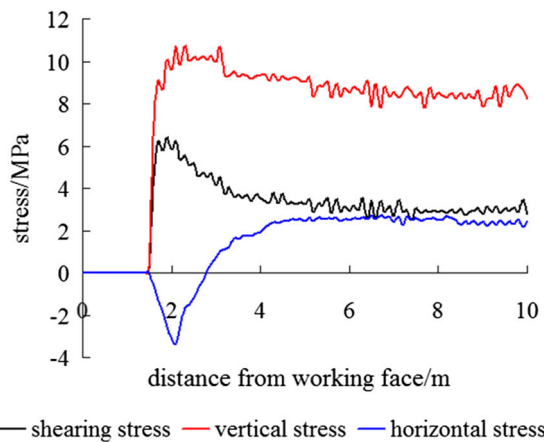
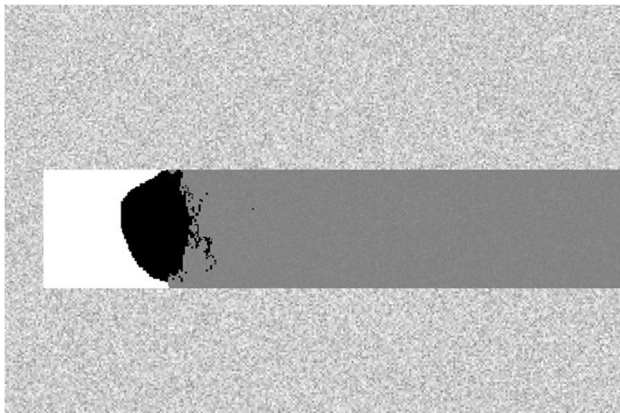


Fig. 13 Stress distribution for the forward working face

fractures gradually expand and connect, gas desorption produces a large gas pressure gap, and the gas moves into a low-pressure zone. Under the coupled effects of the gas pressure and in situ stresses, there is a coal and gas outburst, and many coal blocks are ejected. Then, a new free weak surface forms, and the outburst continues step by step. Once the new weak surface can withstand the comprehensive stress, a new equilibrium state is established, and the outburst is complete. This process is presented in Fig. 11e, f.

Owing to differences in the gas permeability of the coal, the non-uniformity of the coal and the method of the loading stress, the stress experienced by the coal is slightly different in the numerical simulation and physical simulation. The bulk stress is approximately 42–65 MPa in the physical simulation when the outburst occurs. The coal body is subjected to the actions of vertical stress and horizontal stress in the numerical simulation, and the stress is approximately 12.4 MPa when the outburst occurs. If the relationship is based on a three-dimensional in situ stress conversion, the horizontal and vertical stresses in the coal bulk are approximately 50 MPa when an outburst occurs. The entire process of coal and gas outburst was investigated via numerical simulation. An outburst is caused by in situ stress and manual production. The coal strength decreases, a large gas pressure gap forms, and an outburst occurs as a result of the comprehensive stress. The failure zone is an ellipsoid. It is reflected in situ that the failure zone is increased followed by an increase in the coal seam depth. The numerical simulation results demonstrate the four stages of outburst and reveal an approximately ellipsoidal failure zone from acoustic emissions. The numerical simulation reproduces the actual coal and gas outburst phenomenon. Thus, the results of the numerical simulation and physical simulation are in agreement.

4 Conclusions

1. According to the temporal and spatial distributions of acoustic emissions during coal and gas outbursts in physical experiments, the deformation and failure of a coal mass containing methane under three-dimensional stress comprises four stages: initial compression, elastic deformation, plastic deformation and failure. The failure zone has a shape that is similar to that of an ellipsoid. The emission events primarily occur on the weak structural surface at the edge of the ellipsoid. The events gradually increase in number within the ellipsoid, and an outburst then occurs.
2. The gas in a coal mass is desorbed under bulk stress. Then, free gas accumulates, and the gas pressure increases. The gas energy in the coal mass is not released in time, and an outburst occurs. In a regression analysis, the inner gas pressure of a coal mass fits the bulk stress well.
3. The results reveal that the occurrence of a coal and gas outburst depends not only on the gas pressure, in situ stress and physical mechanical characteristics of the coal mass but also on the characteristics of the free weak surface of the outburst. It is more difficult for an outburst to occur when the free weak surface is stronger if all other conditions are the same.

4. The numerical simulation results demonstrate again that the occurrence of a coal and gas outburst depends on the in situ stress, gas pressure and physical mechanical characteristics of the coal mass. A coal mass becomes more fractured, the gas pressure increases, and there is a subsequent increase in the in situ stress. Finally, an outburst occurs, and many coal blocks are ejected under the coupled effects of the gas pressure and in situ stress. The results of the numerical simulation agree with the acoustic emission results for the four stages of outburst and show similar ellipsoidal failure zones.

The present paper focuses on the mechanism of a coal and gas outburst by employing physical and numerical experiments combined with acoustic emission analyses. The results are important in terms of providing a better understanding of the mechanism and preventing coal and gas outbursts.

Acknowledgements This study work is supported by the National Natural Science Foundation of China (21373416, 51304142), the Natural Science Project of Shanxi Province in China (2013021029-3).

References

- Airey EM (1968) Gas emission from broken coal: an experimental and theoretical investigation. *Int J Rock Mech Min Sci Geo Abstr* 6:475–494
- An FH, Cheng YP (2013) An explanation of large-scale coal and gas outbursts in underground coal mines: the effect of low-permeability zones on abnormally abundant gas. *Nat Hazards Earth Syst Sci Discuss* 1:4751–4775
- Beamish BB, Crosdale PJ (1998) Instantaneous outbursts in underground coal mines: an overview and association with coal type. *Int J Coal Geol* 35:27–55
- Butt SD (1999) Development of an apparatus to study the gas permeability and acoustic emission characteristics of an outburst-prone sandstone as a function of stress. *Int J Rock Mech Min Sci* 8:1079–1085
- Chen HD, Cheng YP, Zhou HX, Li W (2013) Damage and permeability development in coal during unloading. *Rock Mech Rock Eng* 46:1377–1390
- Choi SK, Wold MB (2001) A mechanistic study of coal and gas outbursts. In: *Proceedings 38th US rock mechanics symposium*, Washington DC, pp 343–350
- Choi SK, Wold MB (2004) A coupled geomechanical-reservoir model for the modelling of coal and gas outbursts. *Elsevier Geo-Eng Book Ser* 2:629–634
- Hu QT, Zhang ST, Wen GC, Dai LC, Wang B (2015) Coal-like material for coal and gas outburst simulation tests. *Int J Rock Mech Min Sci* 74:151–156
- Huang W, Chen ZQ, Yue JH, Zhang Y, Yang M (2010) Failure modes of coal containing gas and mechanism of gas outbursts. *Min Sci Technol* 4:504–509
- Islam MR, Shinjo R (2009) Numerical simulation of stress distributions and displacements around an entry roadway with igneous intrusion and potential sources of seam gas emission of the Barapukuria coal mine, NW Bangladesh. *Int J Coal Geol* 4:249–262
- Kong XG, Wang EY, Hu SB, Shen RX, Li XL, Zhan TQ (2016) Fractal characteristics and acoustic emission of coal containing methane in triaxial compression failure. *J Appl Geophys* 124:139–147
- Lama RD, Bodziony J (1998) Management of outburst in underground coal mines. *Int J Coal Geol* 35:83–115
- Langmuir I (1917) The constitution and fundamental properties of solids and liquids. *J Am Chem Soc* 5:102–105
- Perera MSA, Ranjith PG, Choi SK, Airey D (2011a) Numerical simulation of gas flow through porous sandstone and its experimental validation. *Fuel* 2:547–554
- Perera MSA, Ranjith PG, Peter M (2011b) Effects of saturation medium and pressure on strength parameters of Latrobe Valley brown coal: carbon dioxide, water and nitrogen saturations. *Energy* 12:6941–6947
- Skoczylas N (2012) Laboratory study of the phenomenon of methane and coal outburst. *Int J Rock Mech Min Sci* 10:102–107
- Skoczyński AA (1953) Communication concerning sudden coal and gas outburst conducted with use of a model in the laboratory of sudden outbursts in the Mining Institute of the Russian Academy of Sciences. *Ugolnik* 10:39
- Sobczyk J (2011) The influence of sorption processes on gas stresses leading to the coal and gas outburst in the laboratory conditions. *Fuel* 3:1018–1023
- Tu QY, Cheng YP, Guo PK, Jiang JY, Wang L, Zhang R (2016) Experimental study of coal and gas outbursts related to gas-enriched areas. *Rock Mech Rock Eng* 9:3769–3781
- Valliappan S, Zhang WH (1999) Role of gas energy during coal outbursts. *Int J Numer Methods Eng* 7:875–895
- Vishal V, Ranjith PG, Singh TN (2015) An experimental investigation on behaviour of coal under fluid saturation, using acoustic emission. *J Nat Gas Sci Eng* 22:428–436
- Wang K, Zhou AT, Zhang JF, Zhang P (2012) Real-time numerical simulations and experimental research for the propagation characteristics of shock waves and gas flow during coal and gas outburst. *Saf Sci* 4:835–841
- Wu SY, Guo YY, Li YX, Yang GL, Niu Y (2009) Research on the mechanism of coal and gas outburst and the screening of prediction indices. *Procedia Earth Planet Sci* 1:173–179
- Xie J, Gao MZ, Yu B, Zhang R, Jin WC (2015) Coal permeability model on the effect of gas extraction within effective influence zone. *Geomech Geophys Geo-energy Geo-resour* 1:15–27
- Xu T, Tang CA, Yang TH, Zhu WC, Liu J (2006) Numerical investigation of coal and gas outbursts in underground collieries. *Int J Rock Mech Min Sci* 6:905–919
- Xue S, Wang YC, Xie J, Wang G (2011) A coupled approach to simulate initiation of outbursts of coal and gas-model development. *Int J Coal Geol* 86:222–230
- Xue S, Yuan L, Wang YC, Xie J (2014) Numerical analyses of the major parameters affecting the initiation of outbursts of coal and gas. *Rock Mech Rock Eng* 4:1505–1510
- Yang TH, Xu T, Liu HY, Tang CA, Shi BM, Yu QX (2011) Stress-damage-flow coupling model and its application to pressure relief coal bed methane in deep coal seam. *Int J Coal Geol* 4:357–366
- Yin GZ, Jiang CB, Wang JG, Xu J (2013) Combined effect of stress, pore pressure and temperature on methane permeability in anthracite coal: an experimental study. *Transp Porous Media* 1:1–16
- Yin GZ, Jiang CB, Wang JG, Xu J, Zhang DM, Huang G (2016) A new experimental apparatus for coal and gas outburst simulation. *Rock Mech Rock Eng* 5:2005–2013
- Zhou AT, Wang K, Wang L, Du F, Li ZL (2015) Numerical simulation for propagation characteristics of shock wave and gas flow induced by outburst intensity. *Int J Min Sci Technol* 1:107–112